Thermal superinsulating silica aerogels reinforced with short man-made cellulose fibers

Julien Jaxel, Gediminas Markevicius, Arnaud Rigacci, Tatiana Budtova

▶ **To cite this version:**

Julien Jaxel, Gediminas Markevicius, Arnaud Rigacci, Tatiana Budtova. Thermal superinsulating silica aerogels reinforced with short man-made cellulose fibers. Composites Part A: Applied Science and Manufacturing, 2017, 103, pp.113-121. 10.1016/j.compositesa.2017.09.018 . hal-01612276

HAL Id: hal-01612276

https://hal-mines-paristech.archives-ouvertes.fr/hal-01612276

Submitted on 5 Apr 2023

HAL is a multi-disciplinary open access archive for the deposit and dissemination of scientific research documents, whether they are published or not. The documents may come from teaching and research institutions in France or abroad, or from public or private research centers.

L'archive ouverte pluridisciplinaire **HAL**, est destinée au dépôt et à la diffusion de documents scientifiques de niveau recherche, publiés ou non, émanant des établissements d'enseignement et de recherche français ou étrangers, des laboratoires publics ou privés.

Thermal superinsulating silica aerogels reinforced with short man-made cellulose fibers

Julien Jaxel[1], Gediminas Markevicius[2,1], Arnaud Rigacci*[2], Tatiana Budtova*[1]

[1] MINES ParisTech, PSL Research University, CEMEF - Centre de Mise en Forme des Matériaux, rue Claude Daunesse, CS 10207, 06904 Sophia Antipolis, France

[2] MINES ParisTech, PSL Research University PERSEE – Centre procédés, énergies renouvelables et systèmes énergétiques, CS 10207, 06904 Sophia Antipolis, France

Corresponding authors :

Tatiana Budtova, email : Tatiana.Budtova@mines-paristech.fr

Arnaud Rigacci, email: Arnaud.Rigacci@mines-paristech.fr

Abstract

Short man-made cellulose fibers (TENCEL® fibers) were used to mechanically reinforce thermal superinsulating silica aerogels. The aerogels were prepared via two drying techniques: ambient pressure drying and with supercritical CO_2, in both cases resulting in monolithic non-brittle materials. The influence of fiber length and concentration on the thermal conductivity and flexural properties of both types of composite aerogels was evaluated. Thermal conductivity in room conditions varied from 0.015 to 0.018 $W.K^{-1}.m^{-1}$; it slightly increased with fiber concentration but remained in superinsulation domain. The importance of fiber percolation concentration for synthesizing monolithic ambient pressure dried composite aerogels was demonstrated. Contrary to neat silica aerogels, non-brittle behavior was observed for composite aerogels regardless of the drying method when reinforced with cellulose fibers. Macroscopic short cellulose based fibers are efficient and easy to use for preparing robust, monolithic, thermal superinsulating aerogel materials.

Keywords

A. Energy materials; A. Natural fibers; B. Thermal properties; B. Mechanical properties; Aerogels.

Introduction

Silica aerogels have been intensely studied over the past decades because of their unique properties which stem from their nano-scale structure. They exhibit low densities (0.050-0.200 $g.cm^{-3}$), high specific surface areas (~ 700 to 1200 $m^2.g^{-1}$) and have extremely low thermal conductivities in ambient conditions (0.013-0.020 $W.K^{-1}.m^{-1}$), making them very attractive for using as innovative thermal insulating materials. However, these extraordinary characteristics come in tandem with poor mechanical properties, resulting in brittle and difficult to manipulate material.

Monolithic silica aerogels are produced via solvent extraction using supercritical (sc) fluids; traditionally CO_2 is used because of mild temperature and pressure conditions required to achieve its supercritical state. Several ways are known to improve silica aerogels' inherent brittleness. One is a "chemical route" which consists of either using modified silica precursors, methyltrimethoxysilane or methyltriethoxysilane instead of standard tetraethoxysilane (TEOS) [1, 2], or via cross-linking of nanostructured silica phase with organic moieties [3, 4]. Another way is a "composite route" which is based on "adding" a reinforcement, such as dispersed fibers (sepiolite [5], or nanofibrillated cellulose [6, 7]), or by building interpenetrated network either with synthetic [8] or natural polymers [9, 10]. In all cases the improvements in Young's modulus and compressive strength come at an expense of the thermal conductivity, as compared to the neat silica aerogel, because of either matrix densification (cross-linking approach) or phonon transport along the "added" more conductive phase (composite approach).

The high cost and technically challenging process of supercritical drying (SCD) drastically limits the use of aerogels [11]. Drying in ambient conditions is thus a topic of active research aiming to preserve silica morphology and properties similar to their SCD counterparts. This is possible thanks to silylation with incondensable moieties as well as a "spring-back" effect allowing re-opening of the pores during final drying stage when stresses are relaxing due to the repulsion of the grafted groups. However, due to the inherent brittleness of pearl-necklace silica network, the initial monolithic shape is not preserved during ambient pressure drying (APD) [12, 13]. To overcome this issue, "composite" approach is used, i.e. using a fibrous mat to "hold together" fragmented silica phase. The resulting flexible products are known as "blankets". This approach is also used to reinforce SCD silica aerogels

which are now produced on the industrial scale [14, 15]. The commonly used fibres in APD silica-based blankets are glass [16, 17] and polypropylene [18]; the best thermal conductivities are around 0.015 – 0.017 W/(m.K) [19]. One publication reports using cellulose nanofibrils which were freeze-dried, impregnated with silica sol and then APD leading to conductivities around 0.023 W/m.K [20].

Recently we proposed a new "green composite" approach which consists of using short (< 2.5 mm) "macro" cellulose fibres for making APD monolithic aerogels [21]. Hydrophobic samples with low thermal conductivity (0.017 W/m K ± 0.001) were obtained. That work reported the feasibility of the approach, however, neither the length of the fibers was varied, nor the mechanical properties of composite aerogels were evaluated. The goal of the present work is to understand the influence of both fiber length (from 2 to 12 mm) and concentration (from 0 to 2 vol%) on APD aerogel density and thermal and mechanical properties. Fiber size distributions were determined for fibers of different lengths with the aim of evaluating fiber percolation concentration. The mechanical properties were tested using 3-point bending approach which takes into account the compression and tensile components thus closely depicting the properties of the material related to its handling. The properties of APD composite aerogels were compared with their SCD counterparts acting here as reference materials.

Experimental

Materials

Solution of prepolymerized oligomers of TEOS, referred to as polyethoxydisiloxane (PEDS), was kindly provided by Enersens, France. The concentration of SiO_2 in ethanol was 20 wt%. Absolute ethanol (99.8%) was from Fisher Scientific; 1,1,1,3,3,3-hexamethyldisilazane (HMDZ), 98%, was from Acros Organics; aqueous ammonium hydroxide ($NH_4.OH$) was from Alfa Aesar. All chemicals were used as received. Water was distillated.

TENCEL® fibers were kindly provided by Lenzing AG, Austria. They are man-made cellulose fibers produced via spinning of cellulose pulp dissolved in N-methyl morpholine N oxide monohydrate (Lyocell process). Their SEM image is shown in Figure 1a. The fibers were precut by Lenzing AG to 2, 6, 8 and 12 mm lengths.

Methods

Preparation of composite aerogels

The detailed description of aerogels' preparation is given in ref. 21. Briefly, fibers were expanded using a knife mill leading to agglomerates' disaggregation. As a result, the volume taken by fiber increased significantly, however, fibers were not broken (see the results on fiber size distribution and comparison with the initial size as given by the provider). The as-prepared fiber network was placed in either cylindrical mold (45 mm diameter and 15 mm height) for the composites which were meant for thermal conductivity measurements or into a rectangular mold (90 mm length, 15 mm wide and 10 mm height) for 3-point bending characterization. PEDS solution was diluted with ethanol to SiO_2 concentration of 8 wt%. The catalyst, 1.6 M aqueous solution of $NH_4.OH$, was added at 7 v/v % of silica sol, and the whole was poured into the molds containing expanded fiber network. Gelation occurred within 25 minutes ± 5 as evaluated by the eye. TENCEL® fiber concentration was varied from 0 to 2 vol%.

Two fiber volume concentrations will be considered: the initial one (as mixed with silica sol), and the final one (in aerogel). As it will be shown in Results section, composites undergo contraction during aging and drying, and thus final fiber volume concentration is slightly higher than the initial one. The final fiber volume concentration was calculated in each case considering fiber weight, sample volume and density of cellulose fibers, 1.5 g/cm^3 (as given by the provider). All composites studied are listed in Table 1 along with their weight and volume concentrations.

The prepared gels were covered with additional ethanol and transferred into a lab oven (Memmert UN30) for aging at 60 °C for 48 h. Hydrophobisation of the gels was performed by immersing them in silylating agent bath (HMDZ) for 72 h at ambient temperature. To remove the traces of HMDZ and by-products, the alcogels were washed several times over a period of three days with absolute ethanol.

The samples were then dried either for 2 h at 140 °C in a lab oven (Memmert ULE 400) to obtain APD aerogels or with sc CO_2 to obtain SCD aerogels (1 L autoclave, pressurization to 80 bar at 37 °C, dynamic washing step with 5 kg of CO_2/h for 1 h, static mode for 2 h, second dynamic washing

for 2 h at the same CO_2 feed rate and pressure, slow isothermal depressurization at a rate of 4 bar/h at 37 °C, for more details see in ref.21). Reference SCD and APD silica aerogels without fibers were prepared from the same formulations and dryings as described above. Representative images of SCD and APD pure silica aerogels and of APD silica-based composite are shown in Figure 1b-d.

Characterisation

The size distribution of TENCEL® fibers was measured after the fiber expansion with the mill using optical microscope Leica DM 4500P equipped with a high-resolution camera 3-CCD (1360 x 1024 pixels) JVC KY-F75U. Sequences of images were taken using Cartograph® (Microvision Instruments) and gathered in 10 mm × 10 mm picture of high resolution (1.33 µm per pixel). Fibers' diameter and length were measured with Archimed® software (Microvision Instruments); at least 100 fibers were analyzed for each fiber length.

Bulk density was calculated from the measurement of aerogel weight (with a Mettler Toledo MS 303TS balance with 1 mg readability) and volume obtained from the aerogel dimensions measured using a caliper.

Specific surface area measurements based on N_2 adsorption BET theory were performed with the ASAP 2020 from Micromeritics. Samples were degassed in vacuum at 100 °C for 10 h before the measurement.

Thermal conductivity was measured with a Fox150 Thermal Conductivity Meter (Laser Comp) equipped with a custom micro-flow meter developed for small samples by CSTB (Hébert Sallée, Grenoble, France) (see details in [22]). Thermal conductivity of the samples was calculated from the heat flow between two plates maintained at 25 °C and 15 °C, respectively.

Scanning electron microscopy (SEM) images were taken using Zeiss Supra 40 FEG-SEM. Samples were coated with a 7 nm platinum layer with a QUORUM Q150T sputter coater before imaging.

3-point bending tests were performed using a Zwick universal testing machine equipped with a 2.5 kN load cell, and a three-point bending fixture based on ASTM D 790-03 testing procedure. The span (distance between two supports) was 60 mm for sample size of 90 mm in length, 15 mm in width and 10 mm in thickness. These sizes were used as far as it was previously reported that for low density

(0.18 g/cm^3) tetramethoxysilane (TMOS) aerogels the ratio between the span and sample thickness should be above 5 for the modulus not to depend on sample geometry [23]. The tests were performed with a loading nose descent rate of 1 mm.min^{-1} and 1000 acquisitions per minute until the bended sample came in contact with the sensor, limiting the final strain to 15-20%.

Results and discussion

Fiber size distribution

TENCEL® fibers are produced via spinning of cellulose solution and thus their composition and diameter D is uniform, 14 μm ± 1, throughout all fiber lengths. Fiber length distributions for fibers pre-cut to 2, 6, 8 and 12 mm and expanded are shown in Figure 2. For all fibers the distributions are monodisperse and rather symmetrical. The mean values averaged in number, L_n, together with the aspect ratio L_n/D, are summarized in Table 2. Median length values were also calculated (see Table 2); they are close to L_n suggesting normal-type size distributions of all fiber lengths. In the following, for the notation of fiber length we shall use 2, 6, 8 and 12 mm for simplicity.

An important characteristic of composites reinforced with fibers is their percolation concentration C^*. It corresponds to the theoretical volume fraction of fibers above which a continuous network is formed. C* can be roughly estimated as the inverse value of the aspect ratio (see Table 2). Composite mechanical reinforcement, as well as viscoelastic properties of molten polymer composites, strongly depend on this concentration.

Pure silica gels break when dried under ambient pressure (Figure 1c). To illustrate the importance of the percolation concentration, APD aerogels with TENCEL® 2 mm fibers of the initial concentration of 0.5 vol% were prepared knowing that C^* for these fibers is 0.72 vol% (Table 2). No monolithic sample was obtained, while with 1, 1.5 and 2 vol% of TENCEL® 2 mm they were macroscopically monolithic. Thus all composite aerogels were prepared with fiber initial volume concentrations above C^* (which is by definition specific for each fiber length as shown in Table 2). It should be noted that because C^* was calculated using L_n value, and fiber length distributions are rather wide, initial fiber concentrations should be at least twice C^* in order to get APD aerogels which are easy to handle.

Samples' shrinkage during processing, bulk density, and morphology

Silica aerogels shrink during the course of preparation, mainly during aging step and, for APD aerogels, also during drying. In the latter case a well-known "spring-back effect" occurs: the gel first contracts due to capillary pressure and then partly recovers its initial volume due to the presence of non-condensable moieties [24, 25]. It is during this step that the pure SiO_2 gel usually loses its monolithicity [26], except some particular cases. Despite the internal fragmentation of silica phase during APD, our composite aerogels obtained with fiber concentration above C* remain macroscopically monolithic (see Figure 1).

Cumulated shrinkage ΔV was used to characterize volume change of aerogels during the whole synthesis process:

$$\Delta V\ (\%) = (1 - \frac{V_{final}}{V_0})100\% \quad (1)$$

where V_{final} is aerogel volume after drying and V_0 is gel volume before aging. Cumulated shrinkage for APD aerogels with TENCEL® of various fiber lengths and an example for SCD aerogel with TENCEL® of 8 mm is presented in Figure 3 as a function of fiber initial volume concentration. No result can be shown for APD pure silica aerogel because the sample was no longer monolithic (see Figure 1c).

Figure 3 shows that cumulated shrinkage decreases with the increase of fiber concentration both for APD and SCD composite aerogels. Without any fibers, the shrinkage of pure silica aerogels is around 17 % ± 1 whereas the addition of 1.5 vol% fibers in the sol drastically limits shrinkage to only 5-6 %. Similar results were already obtained for SC dried TEOS-based aerogels reinforced with sepiolite whiskers [5] or with a mixture of silica, alumina, and aluminaborosilicate fibers [27]. No noticeable influence of fiber length on cumulated shrinkage was observed within the experimental errors (Figure 3).

Bulk density of composite aerogels, as compared to pure silica aerogels, is a result of two oppositely acting effects: i) total mass increase due to the addition of fibers to silica phase, and ii) lower volume shrinkage with the increase of fiber concentration. Figure 4 shows composite aerogel

density as a function of fiber volume fraction in the aerogel for all APD aerogels and for SCD aerogel with 8 mm TENCEL®. Bulk densities of SCD aerogels are very close to those of APD samples. Overall, as expected, composite aerogel density increases with the increase of fiber concentration for both types of drying. Mass increase due to fibers is predominant compared to shrinkage reduction. Ultimately, fiber length does not influence composite density within experimental errors.

The specific surface area S_{BET} of pure silica and composite aerogels was determined using nitrogen adsorption and BET approach. S_{BET} of pure silica APD and SCD aerogels are very similar, around 735 $m^2/g \pm 5$. These values correspond well to what was previously reported in the literature for this type of silica-based aerogels [28]. As shown in refs [5, 21], higher fiber concentration, lower specific surface area because cellulose fibers do not contribute to the surface but increase the mass. No influence of fiber length on S_{BET} was recorded for a fixed fiber concentration; for example, for APD composite aerogels with 1 vol% fiber content specific surface area varied from 600 to 700 m^2/g for all fiber lengths studied.

The morphology of AP dried composite aerogel is shown in Figure 5a,b; SCD composites are very similar. Cellulose fibers form a network "holding" silica phase together (Figure 5a). The latter is a mesoporous network, specific surface area shows and also well-known from literature [29].

Thermal conductivity

The evolution of thermal conductivity of the composites as a function of fiber volume fraction for both for SCD and APD aerogels synthesized with 8 mm TENCEL® is shown in Figure 6. Pure SCD silica aerogel, being monolithic mesoporous material with low density (0.105 g/cm^3), has the lowest thermal conductivity among all samples studied within this work, 0.014 ±0.00042 $W.K^{-1}.m^{-1}$. The increase of fiber volume fraction in SCD composites leads to the increase in thermal conductivity. Similar trend had already been reported for SCD TEOS-based aerogels reinforced with sepiolite of various concentrations [5] or with 2 mm-long TENCEL® fibers [21]. The main reason is that cellulosic fibers are much more conductive than silica aerogel matrix and thus may promote thermal transfer via phonon conduction through fibrous percolating network. The exact thermal conductivity value for TENCEL® is not known, but, for example, thermal conductivity of rayon is 0.054 – 0.070 W/(m.K)

[30]. No clear trend of conductivity vs fibre concentration can be observed for APD aerogels with 8 mm TENCEL®. This is probably linked to the macroscopic cracks generated during evaporative drying which makes the interpretation of conductivity measurements rather delicate. What is important here is that thermal conductivities of APD composite aerogels are very close to the ones of their SCD counterparts.

All the thermal conductivities measured within this study are gathered in Table 1. This large set of values confirms that whatever are the formulations (fiber concentration and length) and drying conditions, the values are very similar (average thermal conductivity of 0.0166 for SCD composite aerogels vs 0.0171 W/m.K for their APD counterparts. APD composites with the lowest and highest fiber lengths, 2 and 12 mm, seem not to perform as well as with 6 and 8 mm fibers. The length of the shortest fibers might not be sufficient to "hold" the silica phase together during ambient pressure drying; these voids do not participate to Knudsen effect and thus increase thermal conductivity. The longest fibers may form too many contacts between themselves thus increasing the solid pathway via more conductive cellulose phase as compared to pure silica aerogel. More results are needed to conclude on the influence of fiber size on thermal conductivity.

Mechanical properties

For the practical applications, such as using silica-based aerogels as thermal superinsulating materials, mechanical properties in general and flexural properties in particular are very important, and thus 3-point bending tests were performed. It was also demonstrated that 3-point bending gives more adequate results in terms of values of flexural modulus *E* and its trend vs aerogel bulk density as compared to the modulus calculated from compression experiments: compressive modulus is usually underestimated and shows $E \sim \rho_{bulk}^{4}$ contrary to flexural modulus with $E \sim \rho_{bulk}^{3}$ [23].

The representative examples of stress-strain curves for APD and SCD composite aerogels are shown in Figure 7a for composites with TENCEL® 8 mm at different fiber concentrations and in Figure 7b for composites with 1 vol% TENCEL® of different fiber lengths. The characteristics for all composites studied are presented in Table 3. Pure silica aerogel is very fragile; it breaks at low flexural strains (see also video in the Supporting Information).

For SCD composite aerogels the addition of fibers leads to the increase of modulus and maximum stress, as expected from the reinforcing effect of fibers (Table 3). Interestingly, despite fracturing of silica phase with increase of strain, SCD composite aerogels do not exhibit brittle failure: TENCEL® fibers keep the matrix intact. Higher TENCEL® concentration for a given fiber length (Figure 7a) and higher TENCEL® length for a given concentration (Figure 7b) leads to a significant improvement of all mechanical characteristics of composites: they exhibit higher modulus and are not fragile compared to pure silica aerogel.

Flexural moduli and maximum strains of APD composites are much lower than those of their SCD counterparts (Table 3). This was expected because of silica phase fragmentation during ambient pressure drying. However, despite the "broken" silica phase, APD composites appear flexible. It may be possible that during mechanical solicitation fragmented silica particles move towards each other and rearrange in space, leading to an apparent flexibility. Here again, despite that silica phase was initially fractionated because of ambient pressure drying, TENCEL® fibers help resisting applied deformation, and composites do not break as pure silica aerogel does.

The influence of final fiber volume fraction on flexural modulus and maximum stress is shown in Figure 8a and b, respectively, for both types of composite aerogels reinforced with TENCEL® 8 mm. As expected, all SCD aerogels show notably higher stress and modulus than APD counterparts. More than three-fold increase in flexural modulus and maximum stress is recorded for composites with just around 2 vol% of cellulose fibers as compared to non-reinforced neat silica aerogel. In addition, both types of composites are much less brittle than their non-reinforced counterpart.

An increase of modulus and compressive strength with the increase of reinforcing fiber concentration is a very well-known phenomenon for composite materials and is widely used in practice. Rather few are known about fiber reinforcement of composite aerogels, and especially of thermal superinsulating aerogels. To the best of our knowledge, only few examples compare composite mechanical properties with its neat matrix: a ten-fold increase in the compressive strength for SCD TEOS-based aerogels reinforced with sepiolite fibers [5], about 20 fold increase in compressive strength for SCD one-pot gelled pectin mixed sodium silicate [9] and about two fold increase in compressive modulus and strength for SCD aerogels based on PEDS impregnated in

silylated freeze-dried nanofibrillated cellulose (NFC) [7]. In all cases mentioned above, the thermal conductivity in room conditions increases by 0.002 - 0.005 W/m.K. What is very important is that in our case the improvement in mechanical properties does not sacrifice thermal conductivity of composites which remains very low, below 0.018 W/(m.K) and, in the best cases, around 0.016 W/(m.K) (Figure 6). In addition, this was achieved with long (several millimeters in length and about 10 microns in width) and much less expensive fiber as compared to nanocellulose. Overall, the moduli of SCD composites obtained in this work are similar or higher compared to those reported for silica-based reinforced SCD aerogels of similar densities [7, 28, 31-34].

Literature reports a strong reinforcement of SCD aerogels when PEDS was impregnated in a wet coagulated cellulose matrix [33], however, cellulose II based aerogels are not thermal superinsulators, and this important property of silica aerogel was lost. Using a similar approach and hydrophobising both phases, some reinforcement was obtained but the thermal conductivity was rather high for superinsulating materials, 0.021 – 0.022 W/m.K [10].

As for APD composite aerogels, rather high value of compressive modulus, 5.4 MPa, was reported for TEOS impregnated into cross-linked and freeze-dried CNF, however, the conductivity was significantly higher than that obtained in this work, 0.023 W/m.K [20] vs 0.016 – 0.018 W/m.K. Another example is APD sodium silicate aerogels reinforced with non-woven silica fibers: they are monolithic but mechanically much weaker, with modulus around 0.3 – 0.5 MPa, and with thermal conductivity strongly increasing with the increase of fiber content, from 0.02 to 0.03 W/m.K [17]. Present mechanical reinforcement can be thus considered as smart and simple.

Conclusions

Monolithic, strong and thermal superinsulating silica aerogels, reinforced with man-made cellulose TENCEL® fibers, were prepared via sol-gel process and drying with two routes: supercritical extraction of the liquid phase with CO_2 and evaporation under ambient pressure at moderate temperature. Volume concentration of fibers was varied from 0 to 2 %, and fiber length from 2 to 12 mm. The influence of fiber length and concentration on composite density, thermal conductivity and mechanical properties via 3-point bending were investigated.

The importance of knowing fiber percolation concentration *C** (and thus of fiber size distribution) was demonstrated as far as no monolithic APD aerogels was possible to prepare below *C**. Cellulose fibers "protect" silica aerogels from volume variations (shrinkage and spring-back) during aging and drying. Bulk densities of composite aerogels slightly increased with the increase of fiber concentration and varied from 0.1 to 0.13 g/cm^3. Specific surface area of SCD and APD composites was high whatever their formulation, around 600 – 700 m^2/g.

Thermal conductivity of SCD composites increased with the increase of fiber concentration, from 0.014 for pure silica aerogel (taken as our reference) to 0.018 W.K^{-1}.m^{-1} for composites with 2.2 vol% of fibers. On the contrary, no clear influence of fiber concentration on the thermal conductivity of APD dried aerogels was observed. The presence of macroscopic cracks makes difficult the exact interpretation of thermal conductivity measurements. The best APD composite aerogels were obtained with TENCEL® 6 mm and 8 mm fibers with thermal conductivities around 0.016-0.017 W.K^{-1}.m^{-1} which is remarkably low for monolithic ambient-dried aerogels.

The presence of cellulose fibers strongly improved the mechanical properties of composites: first, APD aerogels were monolithic contrary to their pure silica counterpart, and second, for both types of composites 2 vol% of fibers induced 3-fold increase in modulus and flexural strength. Both types of composite aerogels were thus much stiffer than SCD pure silica aerogels and also rather flexible. As expected, modulus and maximum strength were lower for APD composites compared to SCD counterparts.

Cellulose fibers provide strong reinforcement of silica aerogels allowing maintaining very low thermal conductivities for both SCD and APD routes. The latter is very attractive as far as it allows avoiding high pressures and sophisticated equipment. Being widely available and cheap, cellulose fibers enable a very simple and efficient way of making very high performance materials.

Acknowledgements

The work was performed in the frame of AEROFIBRES project (contract n°1504C0003) financed by ADEME (French Agency for Environment and Energy Management). Authors are grateful to Lenzing AG, Austria, for providing TENCEL® fibers, and to Enersens, France, for

providing PEDS solutions. Authors thank Pierre Ilbizian for sc CO_2 drying (PERSEE, MINES ParisTech), Suzanne Jacomet for SEM and Gilbert Fiorucci for the help in mechanical experiments (CEMEF, MINES ParisTech).

Electronic supplementary material: The online version of this article (doi:xxxxxxxxx) contains supplementary material, which is available to authorized users.

References

[1] Rao V, Bhagat SD, Hirashima H, Pajonk GM. Synthesis of flexible silica aerogels using methyltrimethoxysilane (MTMS) precursor. Journal of Colloid and Interface Science. 2006;300(1):279-85.

[2] Maleki H, Durães L, Portugal A. An overview on silica aerogels synthesis and different mechanical reinforcing strategies. Journal of Non-Crystalline Solids. 2014;385:55-74.

[3] Meador MAB, Weber AS, Hindi A, Naumenko M, McCorkle L, Quade D, et al. Structure−Property Relationships in Porous 3D Nanostructures: Epoxy-Cross-Linked Silica Aerogels Produced Using Ethanol as the Solvent. ACS Applied Materials & Interfaces. 2009;1(4):894-906.

[4] Zhang G, Dass A, Rawashdeh A-MM, Thomas J, Counsil JA, Sotiriou-Leventis C, et al. Isocyanate-crosslinked silica aerogel monoliths: preparation and characterization. Journal of Non-Crystalline Solids. 2004;350:152-64.

[5] Li X, Wang Q, Li H, Ji H, Sun X, He J. Effect of sepiolite fiber on the structure and properties of the sepiolite/silica aerogel composite. Journal of Sol-Gel Science and Technology. 2013;67(3):646-53.

[6] Hayase G, Kanamori K, Abe K, Yano H, Maeno A, Kaji H, et al. Polymethylsilsesquioxane–Cellulose Nanofiber Biocomposite Aerogels with High Thermal Insulation, Bendability, and Superhydrophobicity. ACS Applied Materials & Interfaces. 2014;6(12):9466-71.

[7] Zhao S, Zhang Z, Sèbe G, Wu R, Virtudazo RVR, Tingaut P, et al. Multiscale Assembly of Superinsulating Silica Aerogels Within Silylated Nanocellulosic Scaffolds: Improved Mechanical Properties Promoted by Nanoscale Chemical Compatibilization. Advanced Functional Materials. 2015;25(15):2326-34.

[8] Wang X, Jana SC. Synergistic Hybrid Organic–Inorganic Aerogels. ACS Applied Materials & Interfaces. 2013;5(13):6423-9.

[9] Zhao S, Malfait WJ, Demilecamps A, Zhang Y, Brunner S, Huber L, et al. Strong, Thermally Superinsulating Biopolymer–Silica Aerogel Hybrids by Cogelation of Silicic Acid with Pectin. Angewandte Chemie International Edition. 2015;54(48):14282-6.

[10] Demilecamps A, Alves M, Rigacci A, Reichenauer G, Budtova T. Nanostructured interpenetrated organic-inorganic aerogels with thermal superinsulating properties. Journal of Non-Crystalline Solids. 2016;452:259-65.

[11] Aegerter A, Leventis N, Koebel MN. Aerogels Handbook: Springer-Verlag New York; 2011.

[12] Mahadik DB, Rao AV, Kumar R, Ingale SV, Wagh PB, Gupta SC. Reduction of processing time by mechanical shaking of the ambient pressure dried TEOS based silica aerogel granules. Journal of Porous Materials. 2012;19(1):87-94.

[13] Wang L-J, Zhao S-Y, Yang M. Structural characteristics and thermal conductivity of ambient pressure dried silica aerogels with one-step solvent exchange/surface modification. Materials Chemistry and Physics. 2009;113(1):485-90.

[14] Fesmire JE. Aerogel insulation systems for space launch applications. Cryogenics. 2006;46(2–3):111-7.

[15] Bardy ER, Mollendorf JC, Pendergast DR. Thermal Conductivity and Compressive Strain of Aerogel Insulation Blankets Under Applied Hydrostatic Pressure. Journal of Heat Transfer. 2006;129(2):232-5.

[16] Kim C-Y, Lee J-K, Kim B-I. Synthesis and pore analysis of aerogel–glass fiber composites by ambient drying method. Colloids and Surfaces A: Physicochemical and Engineering Aspects. 2008;313–314:179-82.

[17] Shao Z, He X, Niu Z, Huang T, Cheng X, Zhang Y. Ambient pressure dried shape-controllable sodium silicate based composite silica aerogel monoliths. Materials Chemistry and Physics. 2015;162:346-53.

[18] Zhang Z, Shen J, Ni X, Wu G, Zhou B, Yang M, et al. Hydrophobic Silica Aerogels Strengthened with Nonwoven Fibers. Journal of Macromolecular Science, Part A. 2006;43(11):1663-70.

[19] Jin C. Aerogels Super-thermal Insulation Materials by Nano Hi-tech. In: Aegerter MA, Leventis N, Koebel MM, editors. Aerogels Handbook. New York, NY: Springer New York; 2011. p. 865-77.

[20] Fu J, Wang S, He C, Lu Z, Huang J, Chen Z. Facilitated fabrication of high strength silica aerogels using cellulose nanofibrils as scaffold. Carbohydrate Polymers. 2016;147:89-96.

[21] Markevicius G, Ladj R, Niemeyer P, Budtova T, Rigacci A. Ambient-dried thermal superinsulating monolithic silica-based aerogels with short cellulosic fibers. Journal of Materials Science. 2017;52(4):2210-21.

[22] Rudaz C, Courson R, Bonnet L, Calas-Etienne S, Sallée H, Budtova T. Aeropectin: Fully Biomass-Based Mechanically Strong and Thermal Superinsulating Aerogel. Biomacromolecules. 2014;15(6):2188-95.

[23] Alaoui AH, Woignier T, Scherer GW, Phalippou J. Comparison between flexural and uniaxial compression tests to measure the elastic modulus of silica aerogel. Journal of Non-Crystalline Solids. 2008;354(40–41):4556-61.

[24] Rao AV, Nilsen E, Einarsrud MA. Effect of precursors, methylation agents and solvents on the physicochemical properties of silica aerogels prepared by atmospheric pressure drying method. Journal of Non-Crystalline Solids. 2001;296(3):165-71.

[25] Rao AP, Rao AV, Pajonk GM. Hydrophobic and physical properties of the ambient pressure dried silica aerogels with sodium silicate precursor using various surface modification agents. Applied Surface Science. 2007;253(14):6032-40.

[26] Scherer GW. Drying gels I. General theory. Journal of Non-Crystalline Solids. 1986;87(1):199-225.

[27] Parmenter KE, Milstein F. Mechanical properties of silica aerogels. Journal of Non-Crystalline Solids. 1998;223(3):179-89.

[28] Wong JCH, Kaymak H, Tingaut P, Brunner S, Koebel MM. Mechanical and thermal properties of nanofibrillated cellulose reinforced silica aerogel composites. Microporous and Mesoporous Materials. 2015;217:150-8.

[29] Pierre AC, Rigacci A. SiO2 Aerogels. In: Aegerter MA, Leventis N, Koebel MM, editors. Aerogels Handbook. New York, NY: Springer New York; 2011. p. 21-45.

[30] The Polymer Data Handbook: Oxford University Press, Inc.; 1999.

[31] Sai H, Xing L, Xiang J, Cui L, Jiao J, Zhao C, et al. Flexible aerogels with interpenetrating network structure of bacterial cellulose-silica composite from sodium silicate precursor via freeze drying process. RSC Advances. 2014;4(57):30453-61.

[32] Cai J, Liu S, Feng J, Kimura S, Wada M, Kuga S, et al. Cellulose–Silica Nanocomposite Aerogels by In Situ Formation of Silica in Cellulose Gel. Angewandte Chemie International Edition. 2012;51(9):2076-9.

[33] Demilecamps A, Beauger C, Hildenbrand C, Rigacci A, Budtova T. Cellulose–silica aerogels. Carbohydrate Polymers. 2015;122:293-300.

[34] Liu G, Zhou B, Du A, Shen J, Wu G. Greatly strengthened silica aerogels via co-gelation of binary sols with different concentrations: A method to control the microstructure of the colloids. Colloids and Surfaces A: Physicochemical and Engineering Aspects. 2013;436:763-74.

Figure legends

Figure 1

TENCEL® fibers (a), pure SCD (b) and APD (c) silica aerogels, and the corresponding APD composite aerogels of diameter around 4.5 cm obtained with 1 vol% TENCEL® of 8 mm length (d).

Figure 2

Fiber length distributions for TENCEL® pre-cut to 2, 6, 8 and 12 mm and expanded.

Figure 3

Cumulated shrinkage vs fiber volume concentration in the sol for APD (open points) and SCD (filled points) aerogels reinforced with TENCEL® of various lengths.

Figure 4

Composite aerogel density as a function of fiber volume fraction for APD (open symbols) and SCD (filled symbols) aerogels with TENCEL® fibers.

Figure 5.

SEM images of APD composite aerogels with TENCEL® 8 mm of final volume concentration 1.1 vol%

Figure 6

Thermal conductivity as a function of fiber volume fraction for APD and SCD aerogels with TENCEL® fibers of 8 mm. The conductivity of APD pure silica aerogel was not possible to measure because of sample fragmentation during drying. Errors, when not shown, are smaller than the symbol; all standard deviations were lower than 0.0015 $W.K^{-1}.m^{-1}$.

Figure 7

Stress-strain curves for pure silica SCD aerogel (red curve 1 on both figures) and for composite aerogels, solid lines for SCD and dashed lines for APD: (a) with TENCEL® 8 mm for fiber concentrations in composite 2.2 vol% (2, 5), 1.1 vol% (3, 6) and 0.6 vol% (4, 7); (b) with TENCEL® at 1 vol% of 12 mm (2, 4) and 6 mm (3, 5).

Figure 8

Flexural modulus and maximum stress for APD (open points) and SCD (filled points) composite aerogels with TENCEL® 8 mm as a function of fiber volume fraction. If errors are not shown, they are smaller than the size of points.

Table 1. Composites prepared and corresponding fibers' concentration. The standard deviations in concentrations were less than ± 0.05 vol% and ± 0.7 wt%.

TENCEL® fiber length	Fiber volume fraction in the sol, vol%	Fiber volume fraction in the aerogel, vol%	Fiber weight fraction in the aerogel, wt%	Thermal conductivity, W/m.K
SCD composite aerogels				
2 mm	1	1.13	14.65	0.0167±0.0002
6 mm	1	1.14	14.76	0.0169±0.0004
8 mm	0.5	0.59	7.86	0.0158±0.0004
	1	1.12	14.64	0.0165±0.0005
	1.5	1.63	20.86	0.0166±0.0004
	2	2.18	26.13	0.0175±0.0001
12 mm	1	1.10	14.80	0.0162±0.0008
APD composite aerogels				
2 mm	1	1.13	15.63	0.0181±0.0005
	1.5	1.63	21.43	0.0175±0.0004
6 mm	0.5	0.51	8.52	0.0175±0.0002
	1	1.11	15.91	0.0174±0.0003
	1.5	1.63	21.64	0.0165±0.0002
	2	2.16	26.95	0.0165±0.0014
8 mm	0.5	0.61	8.33	0.0170±0.0004
	1	1.11	15.29	0.0159±0.0007
	1.5	1.63	21.05	0.0165±0.0004
	2	2.15	26.32	0.0166±0.0006
12 mm	0.5	0.48	8.33	0.0173±0.0005
	1	1.13	15.68	0.0180±0.0007
	1.5	1.60	21.20	0.0181±0.0011

Table 2. L_n, median length, aspect ratio L_n/D and percolation concentration C^* for TENCEL® fibers used for synthesizing composite aerogels.

	L_n, mm	Median, mm	L_n/D	C^*, vol%
TENCEL® 2 mm	1.99 ± 0.22	1.82	142 ± 23	0.72 ± 0.11
TENCEL® 6 mm	5.59 ± 0.45	5.58	399 ± 53	0.25 ±0.03
TENCEL® 8 mm	7.47 ± 1.43	7.49	564 ± 128	0.19 ± 0.08
TENCEL® 12 mm	10.37 ± 1.22	10.60	711 ± 147	0.15 ± 0.03

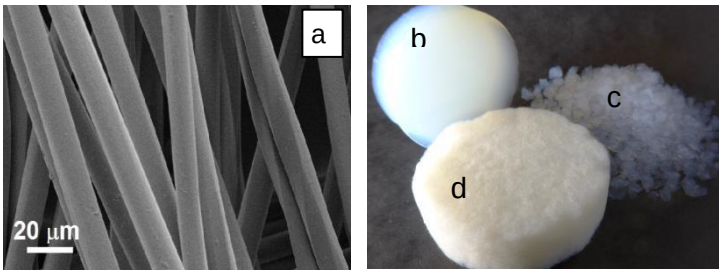

Figure 1

TENCEL® fibers (a), pure SCD (b) and APD (c) silica aerogels, and the corresponding APD composite aerogels of diameter around 4.5 cm obtained with 1 vol% TENCEL® of 8 mm length (d).

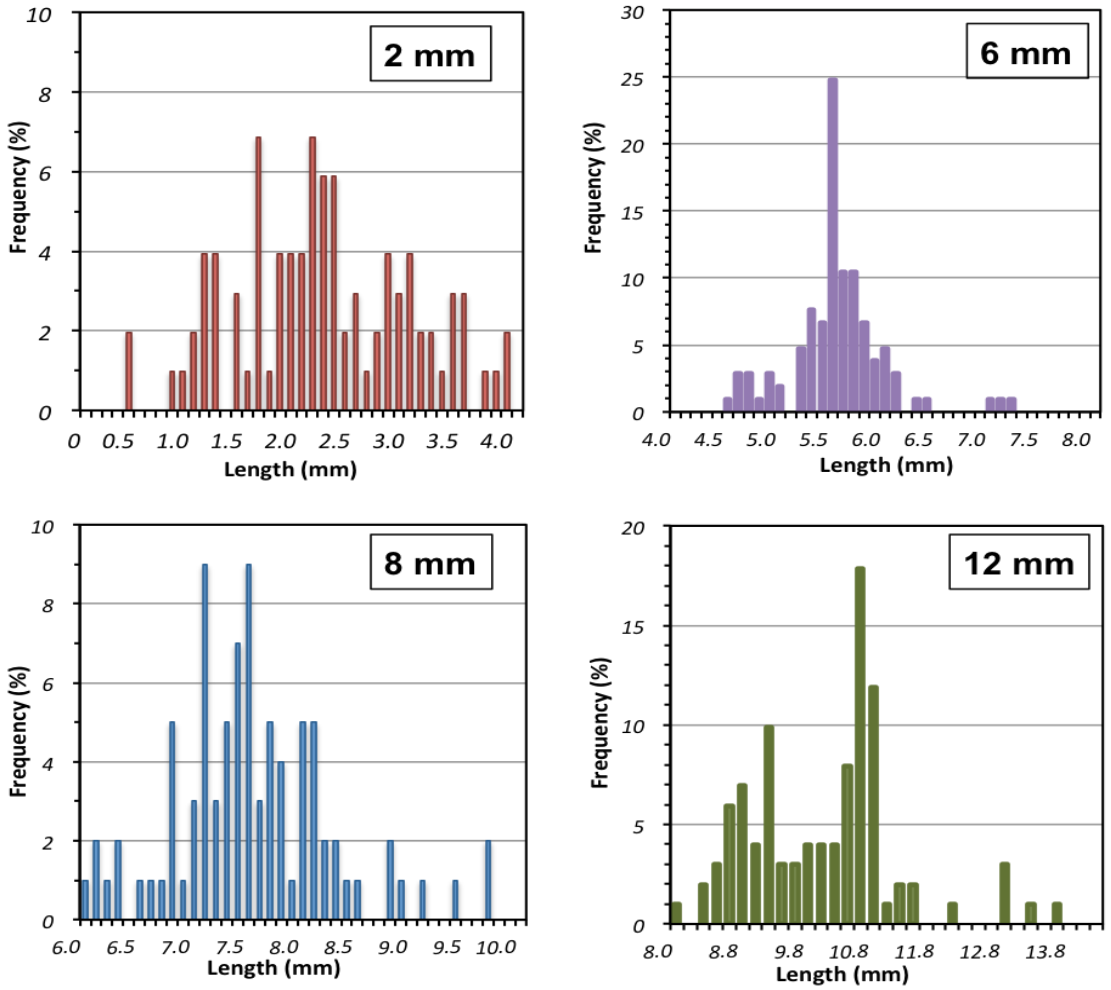

Figure 2

Fiber length distributions for TENCEL® pre-cut to 2, 6, 8 and 12 mm and expanded.

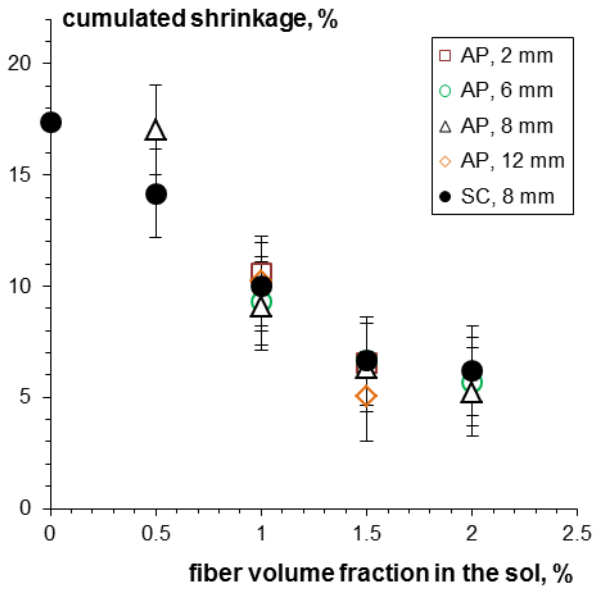

Figure 3

Cumulated shrinkage vs fiber volume concentration in the sol for APD (open points) and SCD (filled points) aerogels reinforced with TENCEL® of various lengths.

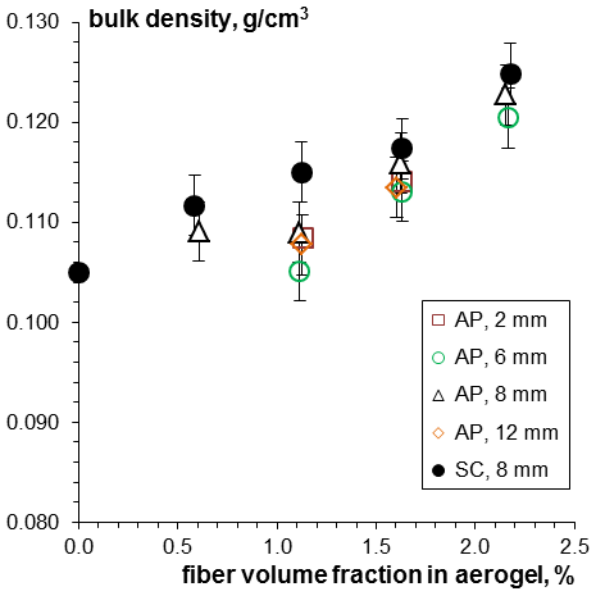

Figure 4

Composite aerogel density as a function of fiber volume fraction for APD (open symbols) and SCD (filled symbols) aerogels with TENCEL® fibers.

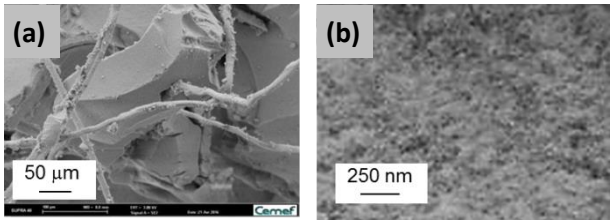

Figure 5.

SEM images of APD composite aerogels with TENCEL® 8 mm of final volume concentration 1.1 vol%

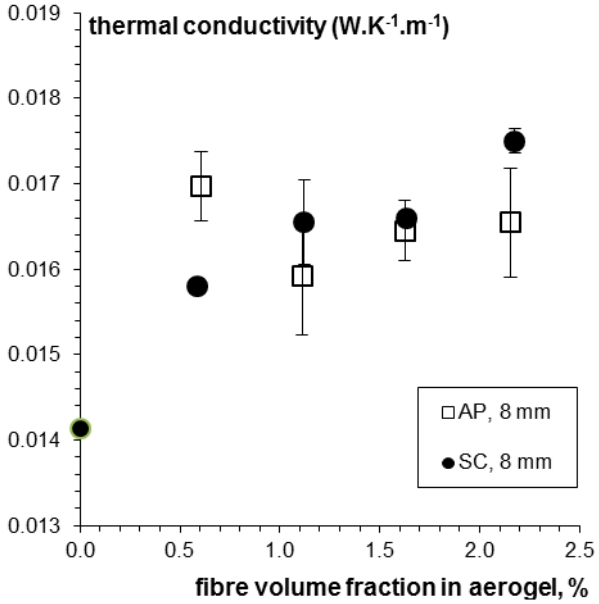

Figure 6

Thermal conductivity as a function of fiber volume fraction for APD and SCD aerogels with TENCEL® fibers of 8 mm. The conductivity of APD pure silica aerogel was not possible to measure because of sample fragmentation during drying. Errors, when not shown, are smaller than the symbol; all standard deviations were lower than 0.0015 $W.K^{-1}.m^{-1}$.

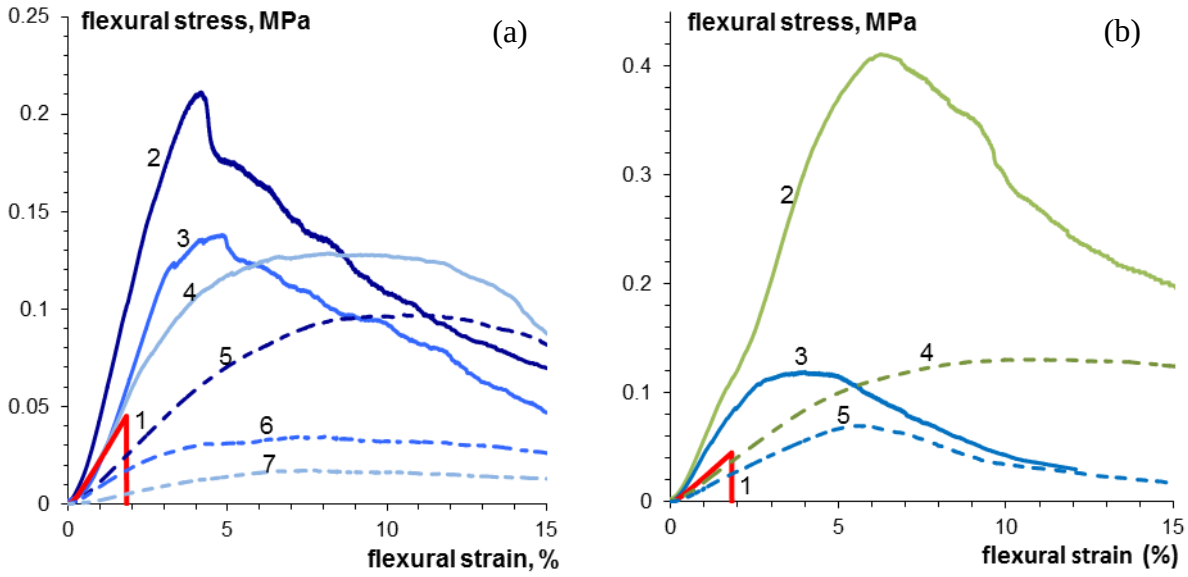

Figure 7

Stress-strain curves for pure silica SCD aerogel (red curve 1 on both figures) and for composite aerogels, solid lines for SCD and dashed lines for APD: (a) with TENCEL® 8 mm for fiber concentrations in composite 2.2 vol% (2, 5), 1.1 vol% (3, 6) and 0.6 vol% (4, 7); (b) with TENCEL® at 1 vol% of 12 mm (2, 4) and 6 mm (3, 5).

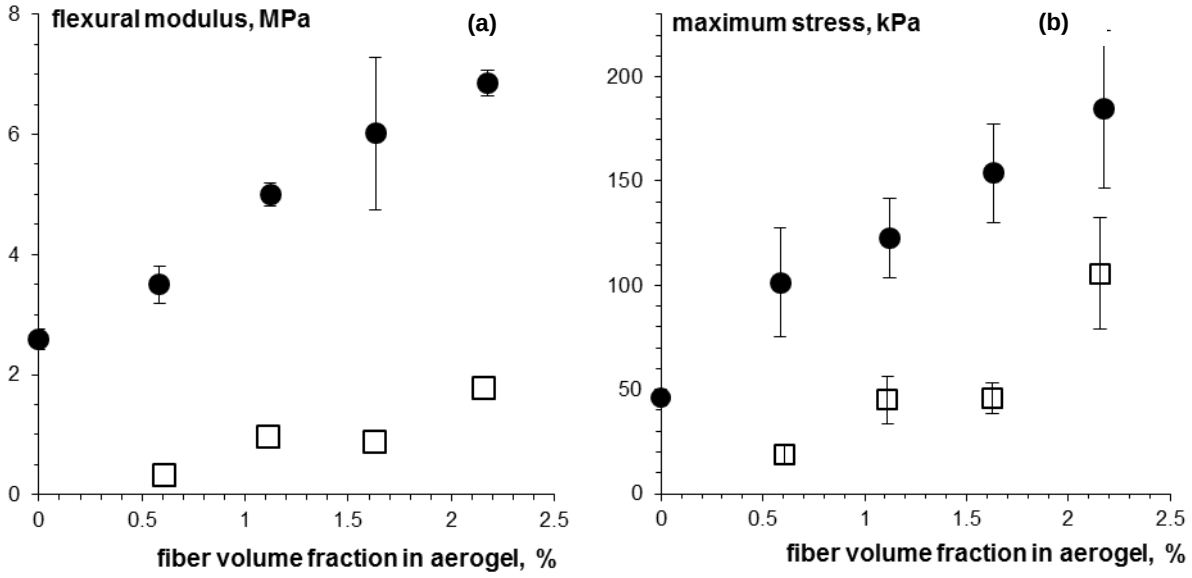

Figure 8

Flexural modulus and maximum stress for APD (open points) and SCD (filled points) composite aerogels with TENCEL® 8 mm as a function of fiber volume fraction. If errors are not shown, they are smaller than the size of points.